

# Evaluation of spatial resolution as a function of thickness for time-resolved optical imaging of highly scattering media

David J. Hall, Jeremy C. Hebden, and David T. Delpy

*Department of Medical Physics, University College London, 11-20 Capper Street, London WC1E, 6JA, England*

(Received 10 July 1996; accepted for publication 25 November 1996)

Previous experimental and theoretical investigations of the utility of time-resolved methods as a means of optical imaging through the human breast have indicated that a spatial resolution of approximately 1 cm is achievable by isolating the shortest path length photons which propagate through the tissue. Studies have also shown that resolution may be improved further by extrapolating the measured distribution using an appropriate model of photon transport. The experiments described here were performed in order to observe the relationship between achievable spatial resolution and the thickness of the medium. For a given time gate, an improvement in the spatial resolution was observed as the object thickness was reduced. Overall, the results indicate that a breast compression of about 1 cm may improve the limiting spatial resolution by as much as 7 mm. Less encouraging is the implication that temporal extrapolation over several orders of magnitude in intensity is required to achieve a comparable improvement in spatial resolution. © 1997 American Association of Physicists in Medicine. [S0094-2405(97)01503-4]

**Key words:** optical imaging, time-of-flight, breast imaging, spatial resolution, temporal extrapolation

## I. INTRODUCTION

During the past decade, biomedical optics has evolved from little more than a curiosity, practiced by a small group of researchers principally involved in other fields, to a large and rapidly expanding discipline in its own right, with an increasing number of scientific journals and international conferences devoted to it.<sup>1-3</sup> One of the most significant goals of this new discipline is the development of a diagnostic imaging modality based on near-infrared (NIR) radiation. This work has been motivated by a number of potential clinical applications, perhaps the most challenging of which is the production of a more effective, less expensive, and safer alternative to x rays as a means of detecting breast disease.

The aspect of optical methods which distinguishes them from existing diagnostic imaging modalities such as x-ray or radioisotope imaging, magnetic resonance imaging, and ultrasound, is the overwhelming dominance of scatter. No light can penetrate more than a few millimeters of breast tissue, for example, without being scattered a large number of times. Thus if optical imaging is to become a viable diagnostic technique, it must rely exclusively on whatever information is encoded in scattered light. The simplest measurement that can be made is the intensity of transmitted scattered light using a continuous wave (cw) source. Initial attempts to image the breast using cw intensity measurements revealed high transmittance of NIR wavelengths at safe exposure levels with high contrast between healthy tissue and some types of tumor.<sup>4,5</sup> However, the very poor spatial resolution (2 cm or worse) demonstrated by breast transillumination methods indicated that they had no utility as a screening method.<sup>5</sup> Fortunately, the search for information encoded in scattered light need not be limited to straightforward measurements of

intensity. The technological breakthrough which has led to the surge in interest in biomedical optics is the ability to record the temporal distribution of light transmitted through tissue, the temporal point spread function (TPSF), or the equivalent in the frequency domain. Time domain measurements, with which this paper is concerned, generally involve a source of picosecond pulses and an ultrafast detector.

Researchers have approached the task of imaging using time-resolved measurements (or their frequency equivalent) in two ways. The so-called indirect approach is based on the assumption that, given a set of measurements of transmitted light between pairs of points on the surface of an object, there exists a unique three-dimensional distribution of internal scatterers and absorbers which would yield that set. Thus imaging becomes a task of solving an inverse problem using an appropriate model of photon transport. A review of the current work on indirect methods has recently been provided by Arridge and Hebden.<sup>6</sup> In principle, the measurements could be of any type, even total transmitted intensity. However, in practice time resolved measurements are considered necessary to avoid the overwhelming dependence on surface interactions that characterize cw measurements. The second, direct approach is based on the principle that photons which are least scattered provide inherently better spatial resolution and contrast since they propagate closest to a straight line through the tissue. Imaging therefore involves appropriate filtering, or "gating," to isolate this transmitted component from the majority of the multiply scattered light. A broad variety of gating techniques have been proposed and tested experimentally.<sup>7</sup> Some methods rely on a fraction of photons being able to propagate without loss of initial coherence<sup>8-11</sup>

or polarization state,<sup>12,13</sup> while other methods gate according to the lengths of the photon paths.<sup>14–20</sup>

This paper represents the third in a series of papers which concern an examination of the spatial resolution performance of time-resolved imaging methods applied to diagnostic imaging, and to breast imaging in particular. As in the previous papers,<sup>21,22</sup> a simple technique borrowed from the field of x-ray imaging is employed to derive quantitative estimates of the spatial resolution achieved when time gating is used to image through a thick slab of material with tissue-like optical properties. The first paper published in 1992 revealed that, as expected, an increase in spatial resolution  $\Delta x$  correlates with a decrease in minimum photon flight time.<sup>21</sup> The experiments also illustrated the degrading effect on the signal-to-noise ratio (SNR) as the width of the time gate  $\Delta t$  is decreased, and an increasing proportion of transmitted light is discarded. Consequently the scarcity of detected photons with the shortest flight times limits the achievable gain in resolution. Research described in a second paper,<sup>22</sup> published in 1995, indicated that straightforward time gating would be unlikely to achieve a spatial resolution better than 1 cm for lesions located furthest from the surface of the breast. This conclusion has been confirmed using imaging studies involving a solid breastlike phantom.<sup>19</sup> The second paper also described an attempt to overcome this limit on spatial resolution performance. This involved improving the estimate of the intensity of short path length photons by fitting a mathematical model to all or part of the TPSF. The model is then used as a noise free estimate of the original data. So-called temporal extrapolation is essentially a SNR enhancement technique which depends on how accurately the model can infer the true population of short path length photons from the available data. Encouragingly, and somewhat surprisingly, this technique demonstrated a significant gain in performance, achieving a spatial resolution of approximately 5 mm through 51 mm of a breastlike medium.

The objectives of the work described in this paper have been twofold. First, to experimentally measure the relationship between the spatial resolution achieved using a time-gated technique and the thickness of the object being imaged. It was anticipated that a study of the likely dependence of resolution and SNR on tissue thickness would indicate the merits, if any, of breast compression for a clinical implementation of the method. The second objective was to confirm or otherwise the effectiveness of the temporal extrapolation technique using a series of separate measurements, and observe the range of object thicknesses over which its application has a significant effect.

## II. THEORY

### A. Evaluation of spatial resolution

As for similar investigations reported previously,<sup>21,22</sup> the spatial resolution measurements described here utilized a method described by Bentzen.<sup>23</sup> This involves measuring the edge response function (ERF) of the imaging system by recording the modulation in signal corresponding to the detection of a sharp boundary between media of highly contrast-

ing transmittance. For a linear system, the derivative of the ERF is the line spread function (LSF). Assuming that the LSF can be represented by a Gaussian distribution, Bentzen provides an approximate analytic expression for the finite integral of a Gaussian consisting of an inverse polynomial. A least-squares fit of this expression to the measured ERF provides a width parameter  $\sigma$  corresponding to the standard deviation of the corresponding Gaussian LSF. It can be shown<sup>21</sup> that, using a common definition of spatial resolution  $\Delta x$  as that corresponding to a 10% response on the modulation transfer function (MTF),  $\Delta x$  is approximately equal to  $2.93\sigma$ . Despite being applied to a technique as obviously nonlinear as time-resolved imaging, so far this method has yielded consistently sensible evaluations of the spatial resolution performance.

### B. Temporal extrapolation method

Temporal extrapolation was originally suggested by Hebden and Delpy,<sup>24</sup> who employed it to improve the resolution of time-gated images of small spheres embedded in a scattering liquid phantom. The technique involves least-squares fitting of a mathematical model of photon migration to all or part of the TPSF in order to improve the estimation of the short path length photons. The model is considered to represent a high SNR estimate of the original data and images are created using the predicted intensities of short path length photons. The argument in support of this method is based on the observation that the transmitted intensity of photons of all path lengths are influenced to some degree by the optical properties along the straight line between source and detector. For a small inhomogeneous region located along this line embedded deep within an otherwise homogeneous medium, the influence of the region on the detected transmitted photons will increase with decreasing flight time. Hence the model fitting provides a means of extrapolating a TPSF known to be smooth and continuous, to shorter flight times where the resolution is higher. Obviously, this technique cannot generate high resolution information from data in which it is not already contained, and therefore relies upon how accurately the model can infer the true population of short path length photons from longer path length photons. Despite the limitations of using relatively simple photon propagation models, previous studies employing temporal extrapolation have so far been highly encouraging.<sup>19,22,24</sup>

## III. EXPERIMENTAL METHOD

### A. Solid edge phantom

One of most important recent developments in biomedical optics research has been the design and production of solid tissue-equivalent phantoms. These have enabled experiments to be performed that would otherwise have been highly impractical if not impossible. Recent research at University College London (UCL) has resulted in the design of two specific recipes,<sup>23,24</sup> each of which can be used to generate solid plastic blocks with optical properties matched to human tissues at NIR wavelengths. In order to study the spatial reso-

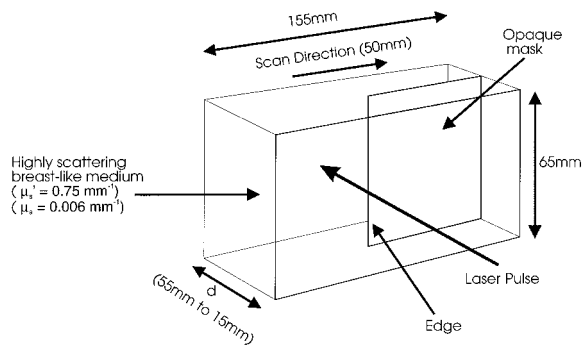


FIG. 1. The variable thickness solid phantom used for measuring the ERF of the imaging system.

lution performance of time-resolved methods as a function of tissue thickness, a phantom was required which (i) contained a sharp opaque boundary from which the ERF could be evaluated, and (ii) had an adjustable thickness. To avoid difficulties associated with having to retain liquids in suitable vessels, it was decided to manufacture a single solid phantom which could be machined to successively smaller thicknesses. The phantom constructed for the experiments described here is illustrated in Fig. 1. It consists of a rectangular block of clear polyester resin in which is suspended a uniform distribution of titanium dioxide particles. The concentration of particles provides a transport scatter coefficient  $\mu'_s$  of about  $0.75 \text{ mm}^{-1}$  at a wavelength of 800 nm, and a small quantity of NIR dye provides an absorption coefficient  $\mu_a$  of about  $0.006 \text{ mm}^{-1}$ . These optical properties fall within the range of reported values for human breast tissues measured *in vivo*.<sup>20</sup> The refractive index at 800 nm is about 1.56.

The phantom material was initially cast into a rectangular slab of dimensions  $155 \text{ mm} \times 65 \text{ mm} \times 55 \text{ mm}$  with a thin rectangular black plastic mask located in the midplane as illustrated in Fig. 1. The mask, which had a measured optical density of about six at 800 nm, was positioned parallel to, and halfway between the two largest sides of the slab, and with the vertical edge located halfway between the two smallest sides. Reduction of the phantom thickness from 55 mm to smaller values was achieved by milling away the two largest surfaces of the phantom by equal amounts so that the opaque mask remained in the midplane. The principal disadvantage of this approach is that, having completed the experiment for a series of thicknesses, the experiment could not be repeated with the same phantom! Nevertheless, because of the time and effort required to manufacture solid phantoms, this method appeared significantly more attractive than having to generate a series of phantoms with different thicknesses. Furthermore, using a single phantom also ensures that the optical properties are always identical for each measurement.

## B. Time-resolved imaging

Time-resolved measurements of the distribution of light transmitted through tissue phantoms are obtained at UCL

using an experimental imaging system described in detail elsewhere.<sup>19,22,24</sup> The principal components of the system are a Ti:sapphire pulsed laser and a streak camera. For the experiments reported here, the laser was operated at a wavelength of 800 nm and with a mean output power of about 1 W. The phantom was illuminated with the beam of picosecond pulses over an area about 3 mm in diameter, and light transmitted through the phantom directly opposite the beam was relayed to the input slit of the streak camera via an optical fiber bundle. The streak images produced by the camera were averaged along the spatial direction to produce intensity versus time profiles, TPSFs, with a temporal resolution which varied between 20 and 30 ps. A reference pulse was also recorded directly from the laser which enabled the absolute time delay produced by the phantom to be determined.

To generate a set of time-dependent edge response functions for each thickness, the phantom was translated horizontally a distance of 50 mm in 1 mm steps and a TPSF was recorded at each position. The vertical edge of the mask intercepted the optical axis at precisely midway through the 50 mm translation. The time over which the transmitted signal was integrated was varied between 2.5 and 150 s, consistent with maintaining a reasonably constant SNR. For a given phantom thickness, the integration time increased as the mask moved across the beam, but integration times became smaller as the thickness of the phantom was reduced. Preprocessing of the data involved performing several standard corrections for various sources of noise and system non-linearity. This included subtraction of the dark current produced by the charge-coupled device mounted on the rear of the streak camera, a shading correction to account for the variation in gain across the face of the detector, and correction for the nonlinear sweep of the streak camera along the temporal axis. The full temporal window recorded by the camera was about 3.5 ns for the larger thicknesses and about 2.3 ns for the smaller thicknesses.

The experiment was repeated for seven different thicknesses from 55 to 25 mm at 5 mm intervals over a period of one month, and then once more for a thickness of 15 mm. The reason for the later addition of a 15 mm measurement is explained in Sec. IV. Each experiment resulted in a set of 51 TPSFs which were processed in several discrete steps as described in detail elsewhere.<sup>22</sup> These include absolute temporal alignment of the TPSFs and removal of a low power background noise component. A recent modification to the experimental system is the addition of a computer controlled digital meter which automatically monitors the laser output power during each experiment. This allows each measured TPSF to be corrected for any small fluctuations in source intensity which would otherwise distort the ERFs generated from the data.

## IV. RESULTS

### A. Spatial resolution evaluated from data profiles

For each phantom thickness a set of ERFs were obtained directly from the corresponding set of TPSFs in a manner

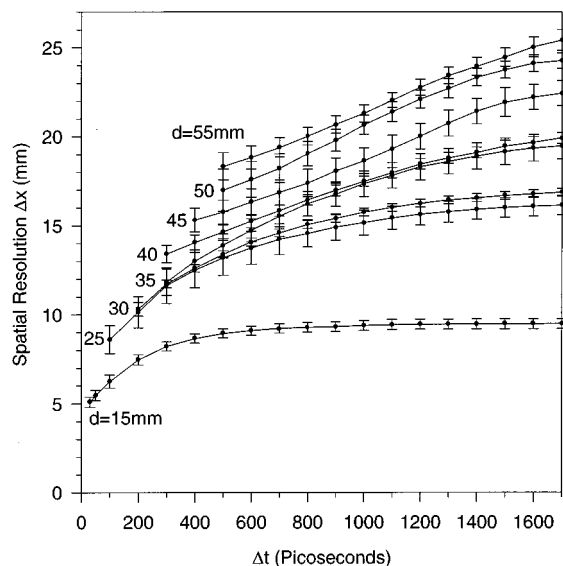


FIG. 2. The estimated spatial resolution as a function of integration time for all phantom thicknesses derived directly from the transmittance data.

identical to that employed for a previous study.<sup>22</sup> This involved numerically integrating the intensity of each TPSF between zero (the time at which an unscattered photon would be detected) and a range of specified integration times. ERFs were generated by displaying the integrated intensity for each integration time,  $\Delta t$ , as a function of the spatial displacement across the edge of the mask. The value of  $\Delta t$  was incremented in 100 ps intervals from 100 to 1700 ps, which was the approximate temporal width of the narrowest TPSF. The Bentzen model was then fitted to each ERF to produce an estimate of the width parameter  $\sigma$  and hence the spatial resolution  $\Delta x$ . The values of  $\Delta x$ , and their associated uncertainties derived from the fitting process are plotted against  $\Delta t$  for each phantom thickness in Fig. 2.

In agreement with previous investigations, Fig. 2 confirms that for a given phantom thickness there is a steady improvement in spatial resolution as  $\Delta t$  decreases. Here, however, it is also observed that for a given value of  $\Delta t$  the spatial resolution is worse for larger thicknesses. The spatial resolution  $\Delta x$  is expected to increase with  $\Delta t$ , converging asymptotically toward the value obtained when all the available light is used. The asymptotic value of  $\Delta x$  corresponds to the resolution expected using cw transillumination methods. For smaller thicknesses the resolution obviously reaches the asymptotic value at a shorter integration time because the TPSF's are correspondingly narrower. Although each curve would be expected to converge toward the same minimum value (equal to the system response function) as  $\Delta t$  decreases, there is a limit below which the integrated intensity becomes too small to evaluate the spatial resolution. Hence the missing data at shorter integration times for larger thicknesses.

## B. Spatial resolution evaluated from a photon transport model

The temporal extrapolation method was again explored as a means of evaluating the spatial resolution performance for integration times over which the recorded flux of photons was below the measurable limit. Several different models of photon transport have been explored for this purpose.<sup>27-29</sup> However, experiments performed so far have indicated that the effectiveness of temporal extrapolation is not particularly sensitive to the choice of model providing that it is able to reproduce the shape of each measured TPSF. Previous implementation of the diffusion model developed by Patterson *et al.*<sup>27</sup> has shown that, providing the four free parameters ( $\mu_a$ ,  $\mu_s'$ , a temporal offset  $t_0$ , and amplitude  $A$ ) are allowed to vary during the fitting process, excellent fits are obtained even in situations where media contain gross inhomogeneities.<sup>19,22</sup>

By employing a protocol identical to that used previously,<sup>22</sup> the diffusion model was least-squares fitted to each of the TPSFs. Fitting was performed over the first 1500 ps of the data. Although the assumption of homogeneity is clearly unrealistic for this experiment, the diffusion model represented the shape of each TPSF very adequately over the fitted range, albeit with fit parameters  $\mu_a$  and  $\mu_s'$  that were not particularly meaningful when the embedded mask was furthest across the optical axis. Typical results achieved by this process are illustrated elsewhere.<sup>22</sup> Models derived from the fitting procedure were used to generate a second set of ERFs for each phantom thickness in a manner identical to that employed for the original TPSFs. The ERFs were acquired for values of  $\Delta t$  at 50 ps intervals in the range from 50 to 500 ps, and at 100 ps intervals from 600 to 1700 ps. Spatial resolution  $\Delta x$  was then evaluated for each new ERF using a least-squares fit to the Bentzen model. The values of  $\Delta x$  and their associated uncertainties are plotted against  $\Delta t$  for each phantom thickness in Fig. 3. The ability to extend the gain in spatial resolution using temporal extrapolation is clearly demonstrated.

Although the uncertainties in the values obtained for the largest thicknesses and the smallest values of  $\Delta t$  were several millimeters, Fig. 3 clearly indicates a convergence of the curves toward a minimum at  $\Delta t=0$ . A number of factors dictate the size of the minimum  $\Delta x$ , and the smallest  $\Delta t$  at which that minimum is reached. First, there is the dependence on the spatial extent of the detector and the illuminating beam. Their contribution to the spatial resolution measurement was evaluated empirically by scanning the beam across the edge of an opaque sheet. Since there was no scattering involved, the total integrated intensity was sufficient to acquire an edge response, which yielded a value of  $\Delta x$  equal to about 1.5 mm. Second, the minimum  $\Delta x$  is limited by the inherent inability to define a value of  $\Delta t$  with greater precision than the temporal resolution of the system. If temporal resolution is denoted by  $\delta t$ , then each value of  $\Delta t$  essentially has a corresponding uncertainty of around  $\pm \delta t$ . Because the number of detected photons rises dramatically with flight time, this uncertainty in  $\Delta t$  will produce an overestimate of

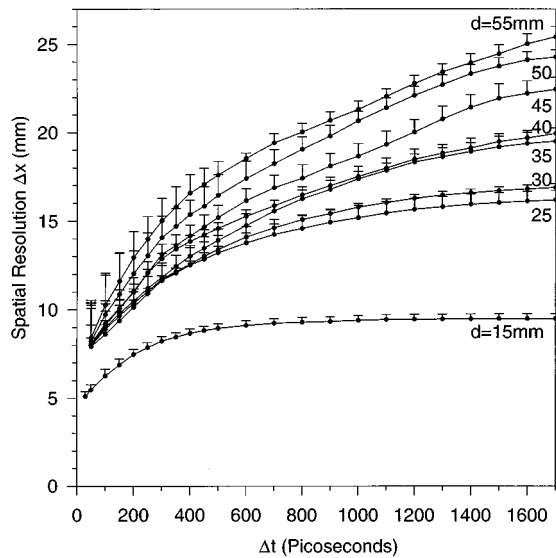


FIG. 3. The estimated spatial resolution as a function of integration time for all phantom thicknesses derived from the least-squares fits of a diffusion model of photon transport.

the spatial resolution  $\Delta x$ . However, this effect will only be significant when  $\Delta t$  is of the order of  $\delta t$ , which was estimated to be never worse than 30 ps overall. A third and far less quantifiable factor which limits spatial resolution is the presence of systematic noise in the data. The potentially most serious source of systematic noise is the temporal nonlinearity, which is an unfortunate feature of data acquired with a streak camera. Despite attempts to reduce its influence, residual temporal nonlinearity certainly produces an additional uncertainty in  $\Delta t$  which is difficult to quantify and which is likely to vary from experiment to experiment. The occurrence of temporal nonlinearity and attempts to correct for its effects are discussed further elsewhere.<sup>19,22</sup> Finally, another factor which almost certainly influences the minimum spatial resolution as exhibited in Fig. 3 is the limited accuracy with which the extrapolation process is able to predict the true intensity of short flight-time photons. The error in the extrapolated values will naturally be largest when the extrapolation is attempted over a greater interval. It is also important to note that a model based on diffusion theory is an inaccurate predictor of photon behavior at short flight times, and therefore the extrapolated intensities for  $\Delta t$  less than about 100 ps are inherently unreliable. Extrapolation errors may be the cause of the apparent convergence of the extrapolated values in Fig. 3 toward a value of around 8 mm at an integration time of 50 ps, which is significantly higher than the limit expected due to other contributing effects.

For phantom thicknesses of 25 mm or larger, there was no measurable flux of photons for integration times less than 100 ps. Thus a further measurement for a thickness of 15 mm was obtained in order to acquire a direct evaluation of the minimum spatial resolution for a value of  $\Delta t$  at or near the inherent temporal resolution of the system. A measurement of the ERF at  $\Delta t=30$  ps yielded a spatial resolution of about 5 mm. This provides a reasonable empirical estimate

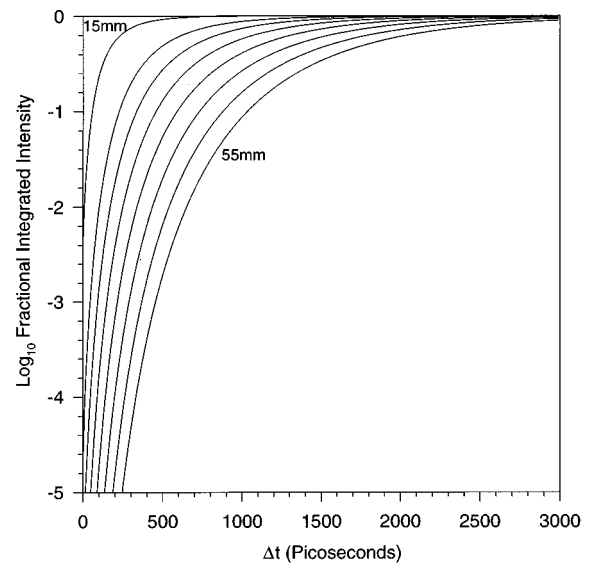


FIG. 4. The normalized integrals of diffusion model TPSFs obtained for homogeneous slabs having the same thicknesses and optical properties as the phantom.

of the minimum spatial resolution achievable with the system when all contributing systematic factors are included, and independent of the extrapolation process. For a linear imaging system, a combination of blurring effects produces a spatial resolution characterized by the geometric mean of the blurring produced by each effect individually. Although the effect of the detector and beam size probably contribute in such a manner to the measured value of  $\Delta x$ , contributions due to uncertainty in  $\Delta t$  or extrapolation errors certainly do not.

### C. Spatial resolution as a function of detected intensity

As has frequently been stressed, the factor which ultimately limits the spatial resolution performance of time-gated imaging is the availability of photons with sufficiently short path lengths through the object. Although experiments have demonstrated the utility of temporal extrapolation to predict the very small intensities of photons having the shortest path lengths, the technique can only hope to be effective over a finite range dependent on the SNR of the original data. The rapid decrease in detected intensity as integration time is decreased is illustrated in Fig. 4. These curves represent the normalized integrals of diffusion model TPSFs obtained for homogeneous slabs having the same thicknesses and optical properties as the phantom described above, in the absence of the opaque mask. Although, as already mentioned above, a diffusion model becomes increasingly unreliable at shorter photon flight times (particularly below 100 ps), these curves indicate the enormous difficulty of measuring or estimating the intensity of light at short integration times for thick objects. This difficulty, and the limited effectiveness of temporal extrapolation, can be emphasized further by using the curves in Fig. 4 to redisplay the spatial resolution mea-

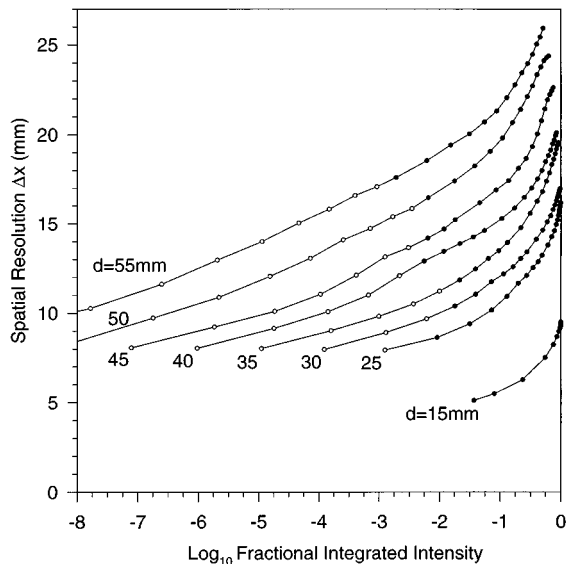


FIG. 5. The spatial resolution measurements shown in Figs. 2 and 3 redisplayed as a function of the relative fraction of integrated intensity obtained from the curves of Fig. 4. (Filled circles=estimates from the experimental data, open circles=estimates from temporal extrapolation.)

measurements shown in Figs. 2 and 3 as a function of the relative fraction of integrated intensity. This is shown in Fig. 5. Spatial resolution estimates obtained only by extrapolation are indicated using open circles, while estimates obtained directly from the data are indicated using filled circles. Error bars, which would be the same as indicated in Fig. 3, are not shown for reasons of clarity. Note that since the integrated intensities were calculated for a homogeneous medium, Fig. 5 can be considered representative of the resolution performance for detection of relatively low contrast embedded features (such as a breast) rather than the phantom containing the large opaque mask. The figure indicates, rather discouragingly, that extrapolation over several orders of magnitude in detected intensity is only rewarded by an improvement in spatial resolution of a few millimeters.

## V. DISCUSSION

There have been several recent theoretical and experimental studies of the spatial resolution performance of time-resolved imaging techniques.<sup>21,22,30-37</sup> Unfortunately comparison of the results of these studies has been hindered by the variety of the definitions for spatial resolution. For example, Mitic *et al.*<sup>30</sup> performed ERF measurements on a 40-mm-thick liquid phantom, defining resolution as the base width of a right-angled triangle fitted to the ERF. A spatial resolution of 12 mm was demonstrated. Studies by de Haller *et al.*<sup>31</sup> involved comparison between time-resolved measurements of *in vitro* breast tissue and Monte Carlo simulations. Instead of measuring spatial resolution directly, the researchers defined the ability to visualize small structures in terms of the image quality index (IQI), which is equal to the diameter of the smallest detectable object. IQI depends on all three of the most fundamental image parameters: contrast,

spatial resolution, and the SNR. In this case, however, spatial resolution was defined in terms of the spread of light on the surface of a slab illuminated from behind at a single point.

A theoretical relationship between spatial resolution and sample thickness has been explored by several researchers. A diffusion-based analysis by Moon *et al.*<sup>32</sup> suggested that for minimum integration times sufficient to collect light above a detectable threshold, the spatial resolution  $\Delta x$  scales with the thickness  $d$  of the sample as  $\Delta x \approx 0.2d$ . A subsequent study by the same researchers<sup>33</sup> inferred that there can be no improvement upon this diffusion limit of spatial resolution for samples thicker than  $\sim 35$  transport lengths by using arbitrarily short time gates. However, once again spatial resolution was defined in terms of the photon distribution on the exit surface. A definition of resolution more consistent with that employed here was used by Joblin,<sup>34</sup> who investigated resolution performance in the specific case of an imaging system involving a gating mechanism with a finite contrast, such as the Kerr cell. Spatial resolution was defined as the full width at half-maximum of the photon distribution at the midplane of a slab using a confocal geometry. Analysis based on the diffusion equation indicated that for some types of gating mechanism there exists a minimum gating time below which the image resolution is not improved. From a consideration of the minimum detectable intensity and the finite contrast ratio of a typical Kerr gate mechanism, Joblin deduced that the limiting resolution would be approximately 20% of the medium thickness.

The most comprehensive theoretical examination of spatial resolution of time-resolved imaging systems has been conducted by Gandjbakhche *et al.*,<sup>35,36</sup> who employed a model based on random walk theory to calculate the LSF of photons as they cross the midplane of a homogeneous slab of finite thickness. A relationship was derived between the spatial resolution (precisely equivalent to that defined here) and the excess time,  $t_{xs}$  by which a photon is delayed by scattering in reaching the detector. Strong support for the model has been provided by previous comparisons with experimental results obtained for media with two different values of  $\mu'_s$  but similar thickness.<sup>37</sup> This comparison involved an assumption that  $t_{xs}$  could be substituted by  $\Delta t$ , which is reasonable over the earliest region of the TPSF where the detected intensity increases rapidly and most of the detected photons will have flight times at or near  $t_{xs} = \Delta t$ . A surprising feature of the model is the suggestion that the spatial resolution is independent of medium thickness. However, whatever contributions to the data there may be from detector temporal nonlinearity, extrapolation error, and other sources of uncertainty in the resolution measurements, Figures 2 and 3 clearly show that the spatial resolution achieved at a given  $\Delta t$  has dependence upon the phantom thickness. This appears to be true even at larger thicknesses and small values of  $\Delta t$  where the approximation of  $t_{xs} = \Delta t$  is most valid.

Overall, the implications of this work for the likely performance of a breast imaging modality based on time gating are moderately encouraging. Figure 3 supports previous claims that subcentimeter spatial resolution is achievable for objects with breastlike properties and thicknesses. It is also

important to note that, using a confocal arrangement as employed here, lesions located nearer to either the detector or source will be imaged with superior spatial resolution. Meanwhile the data presented here can also be used to assess any benefit derived from compression of the breast. Published measurements of the effective attenuation coefficient of breast tissue<sup>38,39</sup> suggest that the total intensity transmitted across the breast will increase by about a factor of 3 for each centimeter of compression. This implies that for a given source and detector sensitivity, a 1 cm compression allows a further 67% of the available transmitted light to be discarded by reducing  $\Delta t$  without a net loss of signal. Figure 5 indicates that the combination of a 1 cm compression and a factor of 3 decrease in the fraction of available signal can improve spatial resolution by perhaps as much as 7 mm. Unfortunately part of this gain will be offset by the requirement for shorter exposure times due to the discomfort caused by significant compression. Less encouraging is the implication from Fig. 5 that extrapolation over several orders of magnitude in intensity is required to obtain a similar gain in resolution. However, it is feasible that the future employment of models able to predict the behavior of the shortest path length photons with more accuracy may yield higher resolution than that currently achieved using a simple model based on the diffusion approximation.

## ACKNOWLEDGMENTS

Support for this research has been generously provided by the EPSRC, the Wellcome Trust, and Hamamatsu Photonics KK. The authors also wish to thank Dr. Amir Gandjbakhche for his encouragement and suggestions which initiated this line of research.

<sup>1</sup> *Photon Migration and Imaging in Random Media and Tissues*, edited by B. Chance and R. R. Alfano (SPIE Bellingham, WA, 1993), Vol. 1888.

<sup>2</sup> *OSA Proceeding on Advances in Optical Imaging and Photon Migration*, edited by R. R. Alfano (Optical Society of America, Washington, DC, 1994), Vol. 21.

<sup>3</sup> *Optical Tomography, Photon Migration, and Spectroscopy of Tissue and Model Media: Theory, Human Studies, and Instrumentation*, edited by B. Chance and R. R. Alfano (SPIE, Bellingham, WA, 1995), Vol. 2389.

<sup>4</sup> P. He, M. Kaneko, M. Takai, K. Baba, Y. Yamashita, and K. Ohta, "Breast cancer diagnosis by laser transmission photo-scanning with spectro-analysis (Report 4)," *Rad. Med.* **8**, 1–5 (1990).

<sup>5</sup> B. Monsees, J. M. Destouet, and D. Gersell, "Light scan evaluation of nonpalpable breast lesions," *Radiology* **163**, 467–470 (1987).

<sup>6</sup> S. R. Arridge and J. C. Hebden, "Optical imaging in medicine. II. Modelling and reconstruction," *Phys. Med. Biol.* (in press).

<sup>7</sup> J. C. Hebden, S. R. Arridge, and D. T. Delpy, "Optical imaging in medicine. I. Experimental techniques," *Phys. Med. Biol.* (in press).

<sup>8</sup> N. H. Abramson and K. G. Spears, "Single pulse-in-flight recording by holography," *Appl. Opt.* **28**, 1834–1841 (1989).

<sup>9</sup> H. Chen, Y. Chen, D. Dilworth, E. Leith, J. Lopez, and J. Valdmans, "Two-dimensional imaging through diffusing media using 150-fs gated electronic holography techniques," *Opt. Lett.* **16**, 487–489 (1991).

<sup>10</sup> J. Reintjes, M. Bashkansky, M. D. Duncan, R. Mahon, L. L. Tankersley, J. A. Moon, C. L. Adler, and J. M. S. Prewitt, "Time-gated imaging with nonlinear optical Raman interactions," *Opt. Photon. News* **4**, 28–32 (1993).

<sup>11</sup> H. Inaba, "Coherent detection imaging for medical laser tomography," *Medical Optical Tomography: Functional Imaging and Monitoring (IS11)* (SPIE, Bellingham, WA, 1993), pp. 317–347.

<sup>12</sup> J. M. Schmitt, A. H. Gandjbakhche, and R. F. Bonner, "Use of polarized light to discriminate short-path photons in a multiply scattering medium," *Appl. Opt.* **31**, 6535–6546 (1992).

<sup>13</sup> S. G. Demos and R. R. Alfano, "Temporal gating in highly scattering media by the degree of optical polarization," *Opt. Lett.* **21**, 161–163 (1996).

<sup>14</sup> L. Wang, P. P. Ho, C. Liu, G. Zhang, and R. R. Alfano, "Ballistic 2-D imaging through scattering walls using an ultrafast optical Kerr gate," *Science* **253**, 769–771 (1991).

<sup>15</sup> L. L. Kalpaxis, L. M. Wang, P. Galland, X. Liang, P. P. Ho, and R. R. Alfano, "Three-dimensional temporal image reconstruction of an object hidden in highly scattering media by time-gated optical tomography," *Opt. Lett.* **18**, 1691–1693 (1993).

<sup>16</sup> S. Andersson-Engels, R. Berg, S. Svanberg, and O. Jarlman, "Time-resolved transillumination for medical diagnostics," *Opt. Lett.* **15**, 1179–1181 (1990).

<sup>17</sup> D. A. Benaron and D. K. Stevenson, "Optical time-of-flight absorbance imaging of biologic media," *Science* **259**, 1463–1466 (1993).

<sup>18</sup> D. A. Benaron, J. P. Van Houten, W.-F. Cheong, E. L. Kermit, and R. A. King, "Early clinical results of time-of-flight optical tomography in a neonatal intensive care unit," *Proc. SPIE* **2389**, 582–596 (1995).

<sup>19</sup> J. C. Hebden, D. J. Hall, M. Firbank, and D. T. Delpy, "Time resolved optical imaging of a solid tissue-equivalent phantom," *Appl. Opt.* **35**, 8038–8047 (1995).

<sup>20</sup> G. Mitic, J. Kolzer, J. Otto, E. Plies, G. Sölkner, and W. Zinth, "Time-gated transillumination of biological tissues and tissuelike phantoms," *Appl. Opt.* **33**, 6699–6710 (1994).

<sup>21</sup> J. C. Hebden, "Evaluating the spatial resolution performance of a time-resolved optical imaging system," *Med. Phys.* **19**, 1081–1087 (1992).

<sup>22</sup> J. C. Hebden, D. J. Hall, and D. T. Delpy, "The spatial resolution performance of a time-resolved optical imaging system using temporal extrapolation," *Med. Phys.* **22**, 201–208 (1995).

<sup>23</sup> S. M. Bentzen, "Evaluation of the spatial resolution of a CT scanner by direct analysis of the edge response function," *Med. Phys.* **10**, 579–581 (1983).

<sup>24</sup> J. C. Hebden and D. T. Delpy, "Enhanced time-resolved imaging with a diffusion model of photon transport," *Opt. Lett.* **19**, 311–313 (1994).

<sup>25</sup> M. Firbank and D. T. Delpy, "A design for a stable and reproducible phantom for use in near infrared imaging and spectroscopy," *Phys. Med. Biol.* **38**, 847–853 (1993).

<sup>26</sup> M. Firbank, M. Oda, and D. T. Delpy, "An improved design for a stable and reproducible phantom material for use in near infrared spectroscopy and imaging," *Phys. Med. Biol.* **40**, 955–961 (1995).

<sup>27</sup> M. S. Patterson, B. Chance, and B. C. Wilson, "Time resolved reflectance and transmittance for the non-invasive measurement of tissue optical properties," *Appl. Opt.* **28**, 2331–2336 (1989).

<sup>28</sup> A. H. Gandjbakhche, G. H. Weiss, R. F. Bonner, and R. Nossal, "Photon path length distributions for transmission through optically turbid slabs," *Phys. Rev. E* **48**, 810–8218 (1993).

<sup>29</sup> J. Kaltenbach and M. Kaschke, "Frequency and time-domain modelling of light transport in random media," in Ref. 11.

<sup>30</sup> G. Mitic, J. Kölzer, J. Otto, E. Plies, G. Sölkner, and W. Zinth, "Time resolved transillumination of turbid media," *SPIE Proc. Biomed. Opt.* **2082**, 26–32 (1993).

<sup>31</sup> E. de Haller, C. Depeursinge, and C. Y. Genton, "Resolution of time-resolved breast transillumination: *In vitro* measurements compared with theoretical predictions," *Opt. Eng.* **34**, 2084–2091 (1995).

<sup>32</sup> J. A. Moon, R. Mahon, M. D. Duncan, and J. Reintjes, "Resolution limits for imaging through turbid media with diffuse light," *Opt. Lett.* **18**, 1591–1593 (1993).

<sup>33</sup> J. A. Moon and J. Reintjes, "Image resolution by use of multiply scattered light," *Opt. Lett.* **19**, 521–523 (1994).

<sup>34</sup> A. Joblin, "Method of calculating the image resolution of a near-infrared time of-flight tissue-imaging system," *Appl. Opt.* **35**, 752–757 (1996).

<sup>35</sup> A. H. Gandjbakhche, R. Nossal, and R. F. Bonner, "Resolution limits for optical transillumination of abnormalities deeply embedded in tissues," *Med. Phys.* **21**, 185–191 (1994).

<sup>36</sup> A. H. Gandjbakhche, R. Nossal, and R. F. Bonner, "Theoretical study of resolution limits for time-resolved imaging of human breast," *Proceedings SPIE Advances in Laser and Light Spectroscopy to Diagnose Cancer*

*and other Diseases* (SPIE, Bellingham, WA, 1994), Vol. 2135, pp. 176–185.

<sup>37</sup>J. C. Hebden and A. H. Gandjbakhche, “Experimental validation of an elementary formula for estimating the spatial resolution for optical transillumination imaging,” *Med. Phys.* **22**, 1271–1272 (1995).

<sup>38</sup>G. Mitic, J. Kolzer, J. Otto, E. Plies, G. Solkner, and W. Zinth, “Time-

gated transillumination of biological tissues and tissuelike phantoms,” *Appl. Opt.* **33**, 6699–6710 (1994).

<sup>39</sup>K. Suzuki, Y. Yamashita, K. Ohta, and B. Chance, “Quantitative measurement of optical parameters in the breast using time-resolved spectroscopy: Phantom and preliminary *in vivo* results,” *Invest. Radiol.* **29**, 410–414 (1994).